D3.3-Fat-IBC Antenna and Transceiver Final Report

Project Number: 965044

Project Acronym: B-CRATOS

Project Title: Wireless Brain-Connect inteRfAce TO machineS

This project has received funding from the European Union's Horizon 2020 research and innovation programme under grant agreement No 965044

Deliverable Information

Project Title:	Wireless Brain-Connect inteRfAce TO machineS (B-CRATOS)
Project Number:	965044
Deliverable Number:	D3.3 Fat-IBC Antenna and Transceiver Final Report
Responsible Partner:	MMG, Uppsala University
Work Package Number and Title:	WP3, D3.3 Fat-IBC Antenna and Transceiver Final Report
Task Number and Title:	T3.1 Fat-IBC Antenna and circuitry
Version:	1.1
Revision Date:	29-04-2023

Dissemination Level: (Public)

Approvals

Name, Org.	Role	Signature	Date
Bappaditya Mandal, UU	Author,WP3 Researcher		27-04-2023
Pramod K.B	Author,WP3 Researcher		27-04-2023
Robin Augustine, UU	Project Coordinator	Robin Augustine	27-04-2023
Rossella Gaffoglio, LINKS	Author, WP3 Researcher		27-04-2023
Giuseppe Musacchio Adorisio, LINKS	Author, WP3 Researcher		27-04-2023
Giorgio Giordanengo, LINKS	Author, WP3 Researcher		27-04-2023

This project has received funding from the European Union's Horizon 2020 research and innovation programme under grant agreement No 965044

Executive Summary

This project report provides a comprehensive analysis of the Fat Intra-Body Communication (Fat-IBC) antenna and its transceiver system, focusing on state-of-the-art design optimization techniques and evaluation methods. The document offers a deep understanding of the fundamental design approach for the Fat-IBC antenna and transceiver system and highlights the innovative strategies employed to maximize its performance.

The project utilizes CST software for the simulation and modeling of the Fat-IBC antenna and tissue models, ensuring accurate and reliable results. The report outlines the findings from these simulations, alongside the experimental studies conducted to validate the simulated results. The report is divided into two main sections: D3.1, which focuses on the initial simulated findings and offers a detailed study of the Fat-IBC antenna in conjunction with the transceiver system; and D3.2, which delves into the optimization process and presents measurement data obtained from tests conducted on a phantom model.

By systematically evaluating the Fat-IBC antenna and transceiver system, the report aims to present a thorough understanding of the technology and its applications. Through simulation and experimental studies, the project endeavors to establish a foundation for future research and development in the field of intra-body communication, paving the way for advancements in medical devices and wearable technology.

This project has received funding from the European Union’s Horizon 2020 research and innovation programme under grant agreement No 965044

Table of Contents

This project has received funding from the European Union’s Horizon 2020 research and innovation programme under grant agreement No 965044

1 Overview

This report overview presents a study focused on Fat Intra-Body Communication (Fat IBC) systems, a promising technology for high-speed data transmission within the human body, and its potential applications in the field of bioelectronics and implantable devices. The study investigates various antenna combinations, including inbody (implanted) and onbody (on the skin) antennas, alongside phantoms and a shielded chamber for evaluating signal coupling and losses through the fat channel.

1.1 Purpose

The main purpose of this BCRATOS report is to explain the requirements and show the final, improved design of the Fat Intra-Body Communication (Fat-IBC) antenna and transceiver system. This report aims to give a clear overview of the benefits of Fat-IBC technology and introduce different types of Fat-IBC antennas and transceiver systems. The results from the antenna-transceiver system will be tested and checked in Task 3.2 to make sure the design meets the specific requirements and works well.

1.2 B-CRATOS Partners

Short Name	**Full Name**
UU	Uppsala Universitet
SINANO	Institut Sinano Association
SSSA	Scuola Superiore di Studi Universitari e di Perfezionamento S’Anna
BRME	Blackrock Microsystems Europe GmbH
LINKS	Fondazione LINKS – Leading Innovation & Knowledge for Society
DPZ	Deutsches Primatenzentrum GmbH
NTNU	Norges Teknisk-Naturvitenskapelige Universitet NTNU

1.3 Responsibilities

U.U serves as the lead beneficiary for Task 3.11 and Deliverable 3.3, holding primary responsibility for the design of the Fat-IBC system that will be utilized in subsequent monkey trail training experiments. The designed transceiver system will undergo testing in Task 3.2 to ensure its effectiveness and suitability for the intended application.

Prof. Robin Augustine (U.U.) assumes the role of scientific coordinator, overseeing the overall project, as well as its scientific and technical aspects. As the B-CRATOS coordinator, Prof. Augustine is responsible for reviewing, approving, and submitting deliverables and reports, ensuring the project remains on track and meets its objectives.

This project has received funding from the European Union’s Horizon 2020 research and innovation programme under grant agreement No 965044

1.4 Definitions

Term	**Description**
B-CRATOS	Wireless Brain-Connect inteRfAce TO machineS project
Fat IBC	Fat Intra-Body Communication
EM	Electromagnetic

1.5 References

[1] N. B. Asan *et al.*, "Intra-body microwave communication through adipose tissue," *Healthc. Technol. Lett.*, vol. 4, no. 4, pp. 115–121, 2017, doi: 10.1049/htl.2016.0104.

[2] N. B. Asan, *Fat-IBC: A New Paradigm for Intra-body Communication*. Digital Comprehensive Summaries of Uppsala Dissertations from the Faculty of Science and Technology 1863, 2019.

[3] N. B. Asan *et al.*, "Data packet transmission through fat tissue for wireless intra body networks," *IEEE J. Electromagn. R.F. Microwaves Med. Biol.*, vol. 1, no. 2, pp. 43–51, 2017, doi: 10.1109/JERM.2017.2766561.

[4] M. Vallejo, J. Recas, P. G. del Valle, and J. L. Ayala, "Accurate human tissue characterization for energy-efficient wireless on-body communications," *Sensors (Switzerland)*, vol. 13, no. 6. pp. 7546–7569, 2013, doi: 10.3390/s130607546.

[5] N. B. Asan *et al.*, "Reliability of the fat tissue channel for intra-body microwave communication," *2017 IEEE Conf. Antenna Meas. Appl. CAMA 2017*, vol. 2018-January, pp. 310–313, 2018, doi: 10.1109/CAMA.2017.8273435.

[6] N. B. Asan *et al.*, "Characterization of the fat channel for intra-body communication at R-Band frequencies," *Sensors (Switzerland)*, vol. 18, no. 9, pp. 1–16, 2018, doi: 10.3390/s18092752.

[7] N. B. Asan *et al.*, "Assessment of Blood Vessel Effect on Fat-Intrabody Communication Using Numerical and Ex-Vivo Models at 2.45 GHz," *IEEE Access*, vol. 7, pp. 89886–89900, 2019, doi: 10.1109/ACCESS.2019.2926646.

[8] D. P. Chandima, K. D. U. I. Dayarathna, H. G. D. A. Jayasinghe, W. K. K. R. Dharmasiri, and H. M. Weerasinghe, "Inductive power transmission, charging and communication for implantable devices," *2017 IEEE Int. Conf. Ind. Inf. Syst. ICIIS 2017 - Proc.*, vol. 2018-January, pp. 1–6, 2018, doi: 10.1109/ICIINFS.2017.8300356.

[9] N. B. Asan *et al.*, "Fat-IntraBody Communication at 5.8 GHz: Verification of Dynamic Body Movement Effects using Computer Simulation and Experiments," *IEEE Access*, pp. 48429–48445, 2021, doi: 10.1109/ACCESS.2021.3068400.

[10] N. B. Asan *et al.*, "Effect of thickness inhomogeneity in fat tissue on in-body microwave propagation," *IMBioc 2018 - 2018 IEEE/MTT-S Int. Microw. Biomed. Conf.*, no. June, pp. 136–138, 2018, doi: 10.1109/IMBIOC.2018.8428872.

[11] E.Chow, M.Morris and P.Irazqui, "Implantable R.F. Medical Devices: The Benefits of High Speed Communication and much Greater Communication Distances in Biomedical Applications." IEEE Microwave Magazines,Vol 14, No 4, pp 64-73, June, 2013.

[12] X.Q.Zhu, Y.X.Guoand, W.Wu, "Miniaturized Dual band and Dual polarized antennas for MBAN Applications.",IEEE Transactions on Antennas and

This project has received funding from the European Union's Horizon 2020 research and innovation programme under grant agreement No 965044

Propagations,Vol 64, 2016.
[13] http://niremf.ifac.cnr.it/tissprop/
[14] Basu, S., Mitra, D., Mandal, B. and Augustine, R., 2020, December. Antenna Based RF Techniques for Intrabody Communication. In *2020 IEEE MTT-S International Microwave Biomedical Conference (IMBioC)* (pp. 1-4). IEEE.
[15] COMSOL Multiphysics, version 5.6. www.comsol.it, 2020.
[16] D. S. Weile and E. Michielssen, "Genetic algorithm optimization applied to electromagnetics: a review," *IEEE Trans. Antennas Propag*., vol. 45, no. 3, pp. 343-53, 1997.
[17] D. Arnaud-Cormos, R. Loison, and R. Gillard, "Fast multistructure method of moments combined with a genetic algorithm (MSMoM/GA) for efficient optimization of printed antennas," *IEEE Antennas Wirel. Propag. Lett*., vol. 6, pp. 172-4, 2007.
[18] P. Soontornpipit, C. M. Furse, and Y. C. Chung, "Miniaturized biocompatible microstrip antenna using genetic algorithm," *IEEE Trans. Antennas Propag*., vol. 53, no. 6, pp. 1939-45, 2005.
[19] Wikipedia. (2023, Feb 26.) IEEE 802.11n-2009.[Online]. Available:https://en.wikipedia.org/wiki/IEEE 802.11n-2009

2 Overview of Fat Intra Body Communication within the Framework of the B-CRATOS Project

The B-CRATOS project aims to harness the potential of Fat Intra Body Communication (Fat-IBC) technology for innovative applications in medical devices and wearable technology. Fat-IBC leverages the conductive properties of body tissues, specifically fat, to facilitate efficient data transmission between implanted or wearable devices within the human body. This unique approach to wireless communication presents numerous advantages and opportunities for advancements in the field.

2.1 Introduction

The human body is composed of diverse tissues, organs, and bone structures, with various body parts such as arms, legs, and torso comprising three key superficial tissues: skin (including epidermis and dermis), fat, and muscle tissue [1]. Orthogonally transmitted signals are attenuated by muscles, making it difficult for them to reach the bone. Fat tissue, which is widely distributed throughout the body and surrounds most major organs, is a more suitable medium for intra-body communication due to its lower losses compared to muscle and skin tissue. Studies have shown that fat tissue is a feasible transmission medium for in-body communication (Fig. 1). Fig. 1(c) illustrates the extraction process for the three-layered tissue model, highlighting the extensive presence of fat tissue around the model and enveloping the majority of the human body's major organs.

The structure formed by fat tissue sandwiched between skin and muscle tissues resembles a parallel plate waveguide. Typically, a parallel plate waveguide consists of two conductors on either side of a dielectric material. The significant contrast in dielectric properties between fat and skin or muscle tissues enables the signal to be confined within the fat layer [2]. Data transmission from various body parts remains a complex process [3], [4]. Fat intra-body

This project has received funding from the European Union's Horizon 2020 research and innovation programme under grant agreement No 965044

communication, or Fat-IBC, involves the use of fat tissue as a communication channel to establish connections between implanted devices separated by a certain distance. Nevertheless, low-frequency propagation (kHz range) is not ideal for IBC, as it leads to lower bandwidth and data rates. Microwave frequencies are heavily attenuated by skin and muscle tissues due to their higher dielectric coefficients [5]. Previous research has shown that IBC is effective for R-band (1.70 to 2.60 GHz) communication [6].

Fat tissue is particularly effective as a communication channel for frequencies around 2.0 GHz [7], offering lower losses and higher bandwidth compared to other tissues. This makes it suitable for supporting functionalities such as cardiac pacemakers, implantable cardioverters/defibrillators (ICD), and neuroprosthetics. It is important to note that Fat-IBC research is still in its early stages, and some applications cannot be realized with current technologies due to limitations such as insufficient bandwidth within the body. Fig. 1 (b) presents one possible scenario for communication between a sensor and the external world. A wireless power receiver, rechargeable battery unit, and wireless communication system can be implanted within the human body [8].

2.2 Benefits of Fat Intra-Body Communication

Microwave communication utilizing fat tissue presents a promising approach for wireless implant-to-implant communication. Establishing a dependable wireless fat channel-based intra-body area network will facilitate the collection of data from multiple implanted medical devices. This enables the development of future implant-based monitoring, controlled drug delivery, and sensor communication systems. Research efforts, such as those considering the impact of blood vessels [7] and incorporating body movements [9], contribute to a more accurate and practical working environment model. Additionally, safety concerns, including the employment of bio-compatible materials for implant antenna development and the calculation of specific absorption rate (SAR), will be explored. Findings from previous research [6] lay the groundwork for creating a novel wireless communication platform for implanted medical devices.

It has been observed that skin and muscle tissues act as conductive layers, with the combination of these high-permittivity materials significantly influencing the transmission signal through the fat tissue by constraining the microwave signal within the fat layer. Studies examining transmission coefficient evaluations and E-field distribution suggest that the presence of skin and muscle tissue enhances microwave propagation through fat tissue. Overall, the presented findings support the proposed technique of employing fat tissue as a novel intra-body communication medium at R-band frequencies.

This project has received funding from the European Union's Horizon 2020 research and innovation programme under grant agreement No 965044

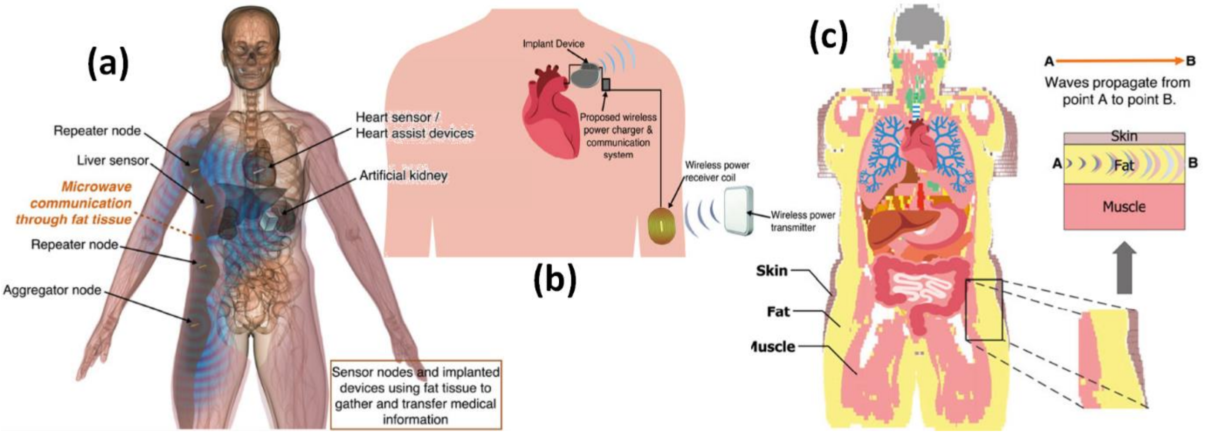

Figure 1. **(a) Conceptual rendering of fat intra-body microwave communication (Fat-IBC) network [3]; (b) Implantable medical device communicates with the external world [2], [8]; and (c) The model shows that the vital organs are surrounded by adipose tissue. The smaller picture of the 3 types of tissues outlines how the intra-body microwave is transmitted through the fat tissue [6].**

2.3 Application of Fat IBC

Fig. 1 (a) illustrates a human body equipped with various implants, such as an artificial kidney, heart sensor, and liver sensor. Wireless communication is a fitting approach to enable interactions among these sensors. In addition to this technique, fat tissue can serve as a medium for microwave communication between the sensors. In situations where the sensors are positioned far apart, signal strength may weaken as it travels through the fat tissue [9]. To improve signal strength, a repeater node can be implemented as an amplification stage. The aggregator node amasses all essential body vital data and conveys information outside the human body [10].

3 Fat IBC antennas

This section will explore the main Fat Intra-Body Communication (Fat IBC) system design, specifically developed for the B-CRATOS project. We will concentrate on the final antennas designed for Fat IBC communications within the B-CRATOS initiative, discussing their design, simulation, and fabrication processes. The B-CRATOS project aims to leverage Fat IBC technology to enable efficient, high-speed communication within the human body. This goal requires the development of specialized antennas that can effectively transmit and receive signals through the fat tissue. To create those antennas, the design process began with a comprehensive analysis of the requirements and constraints of Fat IBC communications. This included understanding the electrical properties of human fat tissue, as well as the frequency range and bandwidth necessary for the desired data rates.

Next, simulations were performed using state-of-the-art electromagnetic simulation software to evaluate and optimize the antenna designs. These simulations focused on the antenna's radiation pattern, impedance matching, and overall performance when interacting with the skin, fat, and muscle tissue medium. Once the simulations were completed and the optimal antenna designs were determined, the fabrication process began. This involved selecting

This project has received funding from the European Union's Horizon 2020 research and innovation programme under grant agreement No 965044

appropriate materials and manufacturing techniques to ensure that the antennas would be biocompatible, durable, and maintain their performance in the demanding in-body environment. The final antennas for Fat IBC communications in the B-CRATOS project were then tested and characterized to validate their performance. This involved measuring their impedance, radiation pattern, and efficiency, as well as conducting practical tests within realistic phantom models to evaluate their ability to support high-speed data communication through fat tissue.

3.1 Introduction

The human body presents a diverse medium for communication, with its various organs possessing distinct properties such as permittivity, permeability, and conductivity. Examples of such organs include the liver, heart, skin, bone, muscle, and fat. A common method for characterizing the human body model is by considering a three-layer body model [11-12]. Intra-body Communication is a multidisciplinary field that encompasses multiple aspects, including antenna design, electromagnetic (E.M.) wave propagation in lossy dielectric mediums, communication between transmitting and receiving antennas, low power consumption, reduced SAR, and more [2]. Antenna design is crucial in establishing reliable communication links while also ensuring biocompatibility and addressing human safety concerns.

In this section, we will explore intra-body communication by focusing on the use of fat tissue. We will present various types of Fat Intra-Body Communication (Fat IBC) antennas. An approach for intra-body communication involving transmitting (Tx) and receiving (Rx) antennas is presented, and the transmission characteristics of microwave signals through these layers are modeled.

3.2 Dual ring shape Fat IBC Antenna

Ring shape rigid antenna has been designed Fat IBC communication. This antenna has been designed on very low-cost FR4 material, which dielectric constant, loss tangent and height is 4.4, 0.02 and 1.6, respectively. The antenna has been encapsulated inside the PDMS. We have simulated the antenna placed on three layers of the human tissue model and optimized the antenna to operate at 2.45 GHz. Fig. 2 shows the antenna geometry, fabricated structure, and simulated reflection coefficient plot. Fig. 2 shows the basic schematic diagram antenna prototype and the three-layer tissue model.

This project has received funding from the European Union's Horizon 2020 research and innovation programme under grant agreement No 965044

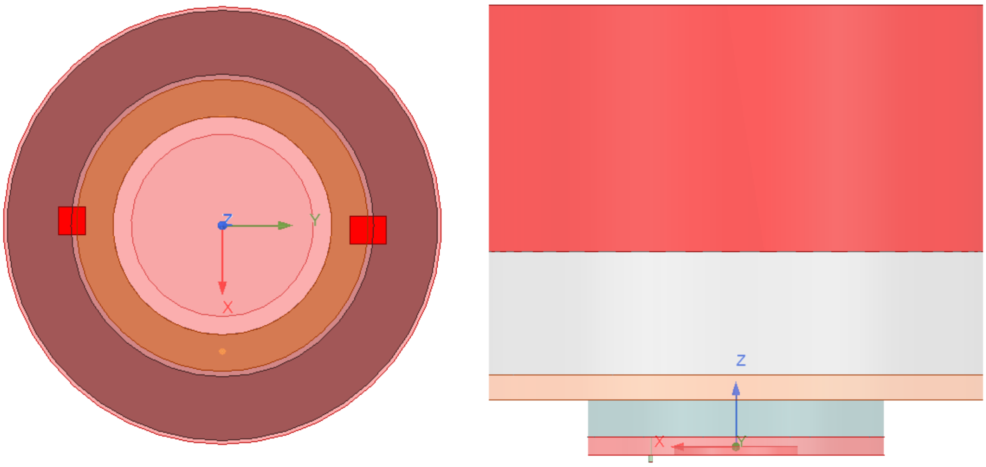

Figure 2. **Schematic diagram of Ring-Shaped Fat-IBC antenna with a three-layer model (Details dimension is not provided due to confidentiality)**

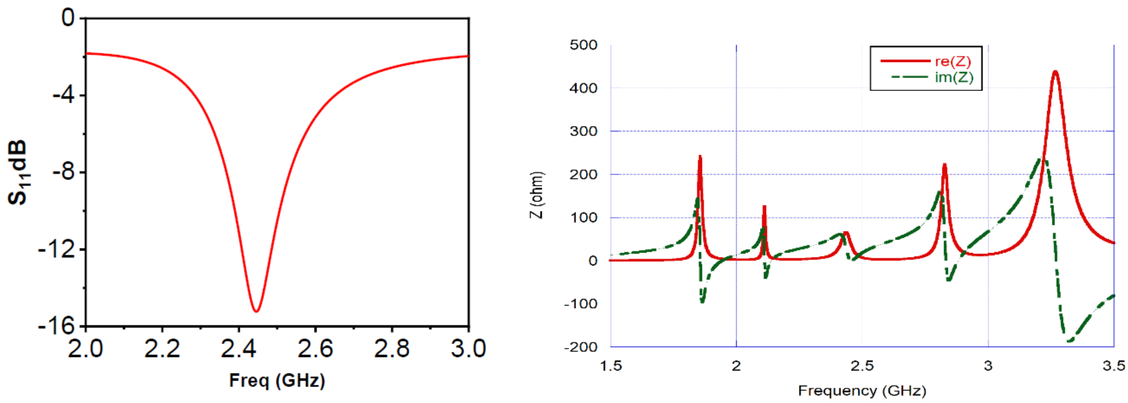

Figure 3. **Reflection coefficient and input impedance plot of Ring-Shaped Fat-IBC antenna with three-layer tissue model**

Fig. 3 shows the antenna's simulated reflection coefficient and input impedance plot placed on the skin layer. The antenna has been optimized to work at 2.45GHz and the simulated input impedance at the desired frequency near about 50 ohm.

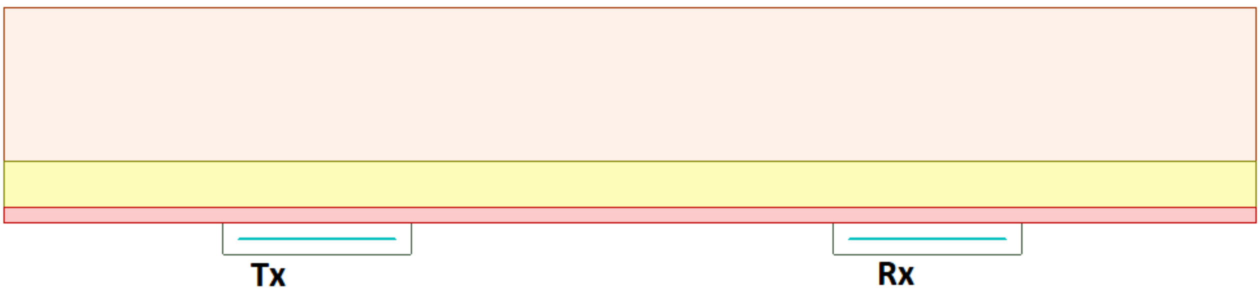

Figure 4. **Fat Channel characterization at different distance**

This project has received funding from the European Union's Horizon 2020 research and innovation programme under grant agreement No 965044

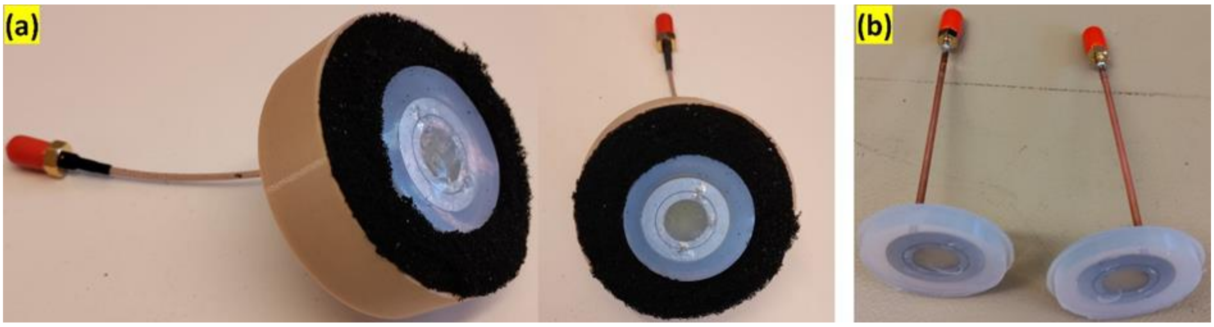

Figure 5. **Pictures of proposed BCRATOS antenna (a) Antenna with microwave absorbers for isolation, and (b) Fabricated antenna.**

We have simulated and characterized the fat channel using a ring-shaped antenna placed on the skin tissue at different distances like 10 cm, 20cm, and 30 cm. In fig. 4 shows the Tx and Rx node at a certain distance. We have fabricated a circular-shaped antenna, depicted in Fig. 5, specifically designed to optimize performance. In conjunction with the antenna, we utilized advanced 3D printing techniques to create a custom housing embedded with an absorber material. This strategic combination effectively mitigates rearward radiation, thereby ensuring that data transmission occurs predominantly through adipose tissue, thus enhancing the overall efficiency and performance of the system.

3.3 Epidermal antenna solutions for Fat-IBC

Printed Monopole Antenna Solution: The proposed solution is a monopole antenna with a triangular-shaped radiating element and a trimmed back-placed ground plane, printed on a substrate of Rogers RT/duroid 6010.2LM (ε_r=10.7,σ=0.0033 S/m) with a thickness t fixed to 0.635 mm. As shown in Fig. 6, the antenna is embedded into a rigid brick, made of a material with relative permittivity ε_r=10, and placed on three layers with different dielectric properties, mimicking the skin, fat, and muscle tissues of the human body. The brick with high permittivity has been added to the antenna structure to improve the radiation coupling into the body. The geometrical parameters reported in Fig.7 (left picture) have been optimized in CST MWS to minimize the reflection coefficient (|S_11 |)) and maximize the transmission coefficient (|S_{21} |) of a TX-RX link with length d=10 cm at the operating frequency f=2.44 GHz. It is important to note that the R_X antenna of the link is simply obtained from the TX one by mirroring it with respect to the transverse xz plane.

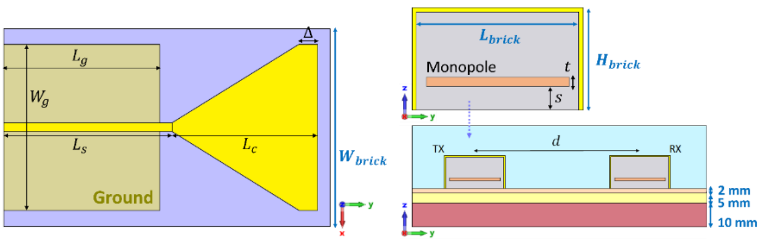

Figure 6. **Left: Sketch of the printed monopole antenna with the triangular-shaped radiating element; right top: monopole antenna embedded into a rigid brick and surrounded by a metal cover; right bottom: optimized link.**

This project has received funding from the European Union's Horizon 2020 research and innovation programme under grant agreement No 965044

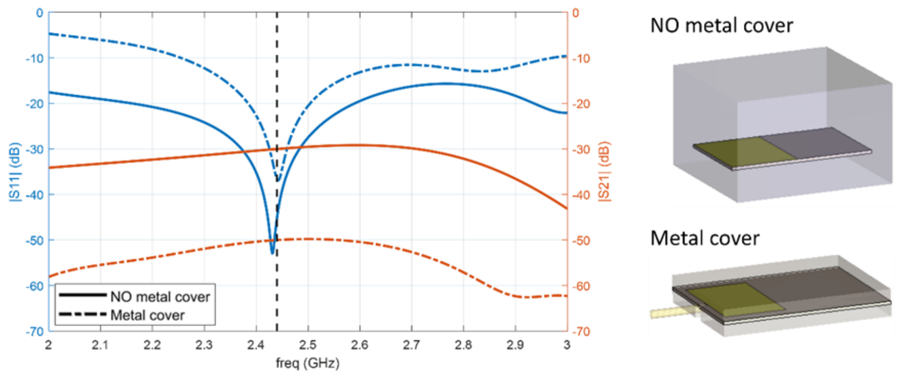

Figure 7. **Left: Simulated S-parameters as a function of frequency for a link distance d=10 cm and different optimized configurations; right: optimized structures, without (top) ad with (bottom) the metal cover.**

The optimization of the different geometrical parameters has been repeated for two different layouts, i.e., with and without a metal cover surrounding the brick to reduce the radiation coupling through the air and confine as much as possible the radiation in the subcutaneous fat layer (to prove the Fat-IBC). The simulated results for the two optimized structures are reported in Fig. 7.

As can be observed, when a metal cover is added, a significant reduction of the transmission coefficient is observed. In this case, the propagation through the air is minimized by the presence of the metal layer.

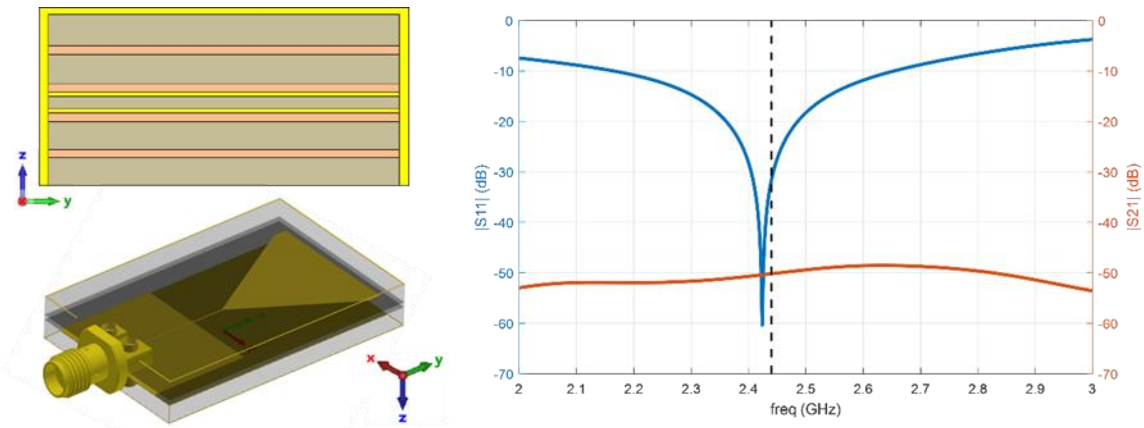

Figure 8. **Left: stack-up (top) and perspective view (bottom) of the realizable version of the monopole antenna solution; right: simulated S-parameters for a link distance d=10 cm.**

L_g	W_g	L_s	L_c	Δ	s	t
14.480	22.816	19.083	17.760	2.069	2.900	0.635

Table 1: Optimized dimensions in mm for the realizable embedded monopole antenna

A slightly different stack-up was considered to build the antenna using commercial PCBs with high permittivity ε_r. As depicted in Fig. 8, more layers are bonded together in this configuration to achieve a sufficient thickness H_{brick} of 6.435 mm. The dielectric used for both the monopole

This project has received funding from the European Union's Horizon 2020 research and innovation programme under grant agreement No 965044

substrate and the surrounding layers (forming the brick) is the Rogers RO3010 (ε_r=11.2, tanδ=0.0021), while the material used to bond the different layers together is the SpeedWave300 (ε_r=3.16, tanδ=0.0021). The geometrical dimensions of the antenna have been optimized using a TX-RX link with length d=10 cm and thicknesses 2, 5, and 10 mm for the skin, fat, and muscle layers, respectively. With reference to Fig. 6, the overall dimensions of the brick were found to be 30×42×6.435 mm3, while the other optimized dimensions are reported in Table 1. To minimize the radiation coupling through the air, the brick is completely covered by a Copper layer (see Fig. 3 (top left)). The resulting simulated S-parameters for a TX-RX link with length d=10 cm are reported in Fig. 8 (right).

3.4 GA-Optimized Antenna Solution

The other structure proposed is a simple patch antenna, where the metal patch has been optimized using a genetic algorithm (GA) interfaced with a full-wave simulation of the structure (performed in COMSOL Multiphysics). The implemented procedure can be described as follows. The metal patch of the antenna is first divided into $(N_x \times N_y)$ square pixels, with $N_x = N_y = 22$. In the logic of the GA, each independent metal pixel is associated to a bit, with 1 and 0 signaling the presence and the absence of metal, respectively. In this way, each sequence of $(N_x \times N_y)$ bits represent a single individual, which corresponds to a particular configuration of the considered antenna. The fitness function (*FF*) for each individual is then computed by means of a full-wave simulation performed in COMSOL, using a TX-RX link, where the second (RX) antenna is obtained by simply mirroring the first one. The considered *FF* function is:

$$FF = \max_f(-|S_{21}|_{\mathrm{dB}} + |S_{11}|_{\mathrm{dB}}) \text{ with } f \in \{2.41,\ 2.44,\ 2.47\}\ \mathrm{GHz}$$

aimed at maximizing the transmission and minimizing the reflection coefficient within a sufficiently large bandwidth. As depicted in **Error! Reference source not found.**, a geometric s ymmetry has been enforced on the structure, reducing the total number of pixels by half.

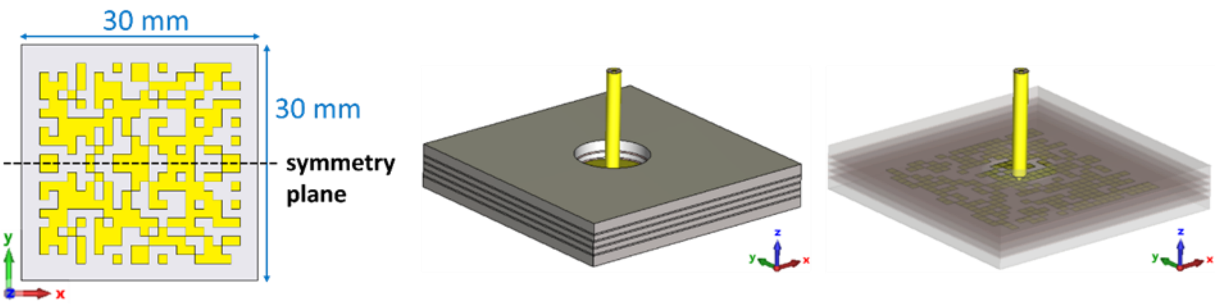

Figure 9. ***Left*: pixeled patch of the GA-optimized antenna solution; *right*: perspective view of the antenna structure, covered by a metal layer and fed in the center by a coaxial cable.**

This project has received funding from the European Union's Horizon 2020 research and innovation programme under grant agreement No 965044

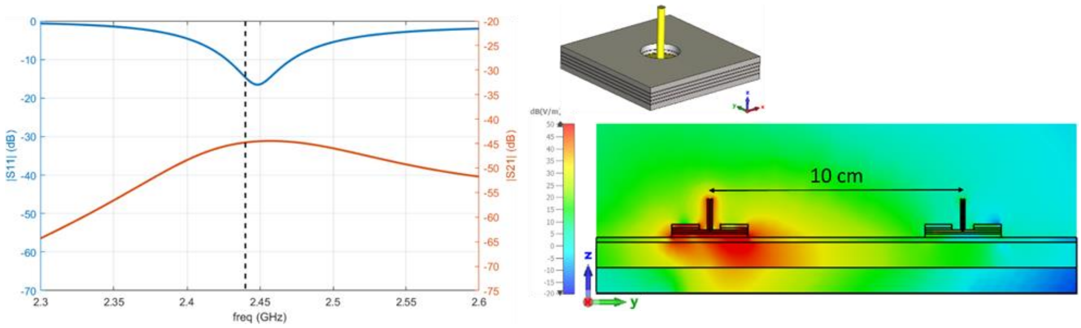

Figure 10. **Left: Simulated S-parameters for a link distance d=10 cm and a Fat thickness of 10 mm; right: electric field magnitude through the different layers.**

The considered optimized antenna is printed on a substrate of Rogers RO3010 ($\varepsilon_r = 11.2$, $\tan\delta = 0.0021$) and surrounded by layers of the same material, with a stack-up similar to the one reported for the monopole antenna solution (see Fig. 9, *top left*) and a total height $H_{brick} = 5.165$ mm. Moreover, the antenna is covered by a metal layer to reduce the radiation coupling through the air and positioned on three layers of skin, fat, and muscle with thicknesses 2, 10, and 10 mm, respectively. Fig.10 reports the simulated S-parameters (*left*) and the electric field magnitude (*right*) for a link distance $d = 10$ cm. As can be observed, the radiation coupling through the fat layer is stronger than through the air.

The manufacturing of both the antenna structures (printed monopole and GA-optimized antenna) is almost completed in order to allow the experimental testing on the tissue phantoms.

4 Fat IBC Transceiver

In this section, we will discuss about the transceiver system for B-CRATOS. This is the preliminary proposal for the Fat IBC transceiver system. The main objective of the transceiver is to establish a bidirectional communication channel between the neural readout board and the AI board (as schematically depicted in Fig. 11), providing a reliable and fast communication channel within the subcutaneous fat layer. To deal with this problem, different solutions have been formulated and are reported below.

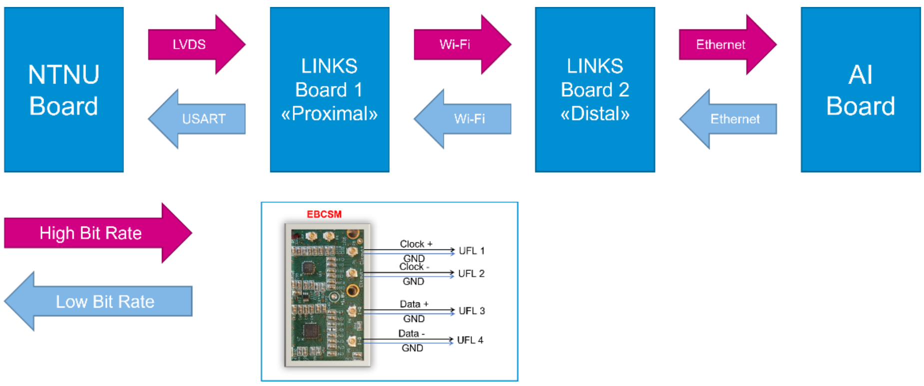

Figure 11. **Block diagram of the system.**

This project has received funding from the European Union's Horizon 2020 research and innovation programme under grant agreement No 965044

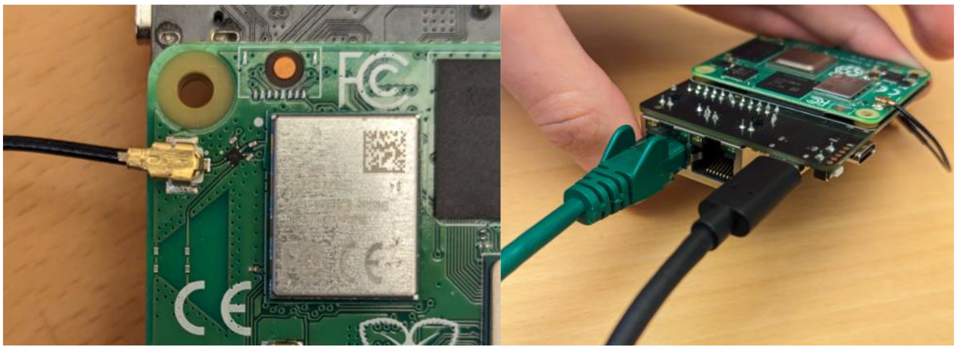

Figure 12. **B205-Raspberry Pi Compute Module 4(CM4) for the fat-IBC wireless communication**

We employ the integrated WiFi chip of a Raspberry Pi Compute Module 4 (CM4) for Fat Intra-Body Communication (Fat-IBC) wireless communication. The board features a U.FL antenna connector (Fig. 12), to which we attach a U.FL to SMA adapter. Fig.12 displays the U.FL antenna connector on the CM4.

The CM4 is mounted onto the "DFRobot IoT Router Board," which offers two Ethernet ports, two USB-C ports (as shown in Fig.13), and a pair of jumpers for managing EEPROM and boot mode. Both jumpers should be set to 0 during standard operation. Fig.12 illustrates the connections on the CM4.

The Ethernet port situated near the corner serves as the primary port. The other port necessitates additional configuration and is not enabled by default. The USB-C port on the back (adjacent to the Ethernet ports) delivers power to the board. Meanwhile, the other USB-C port can flash the onboard eMMC storage when the RPIBOOT jumper is set to 1. Following the development of the antennas, the system operates in the ISM band and, more specifically, with a central frequency of 2.45GHz, the uplink and downlink data streams. Given the limitations imposed on the transmitted power level and the heavy losses estimated for the propagation in the Fat IBC channel, we carefully evaluated the link budget, ensuring that it is possible to establish a reliable link over distances spanning a few tens of centimeters.

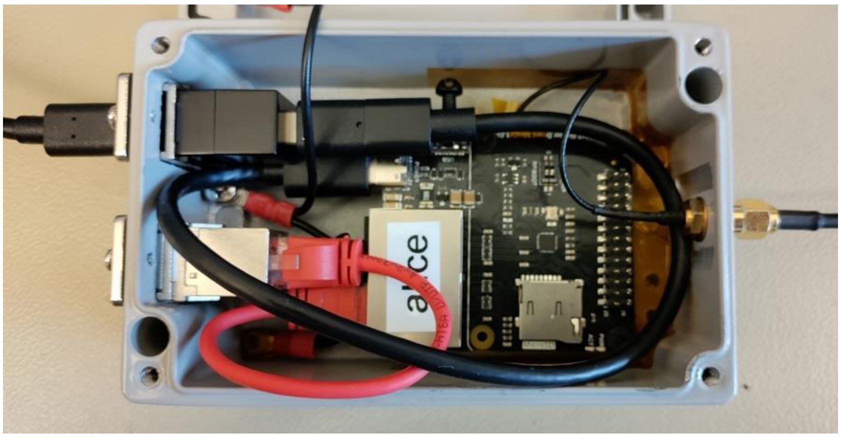

Figure 13. **B205- Raspberry Pi Compute Module 4 units (CM4102008) used for the IEEE 802.11n link.**

In order to assess the feasibility of utilizing Fat-IBC for high-speed data transmission, we employed in-body (implanted) antennas, topology-optimized planar antennas (TOPA), and two Raspberry Pi Compute Module 4 units (CM4102008). This specific Raspberry Pi model

This project has received funding from the European Union's Horizon 2020 research and innovation programme under grant agreement No 965044

features a wireless module based on the Cypress Semiconductor CYW43455, which, in contrast to the wireless module on the standard Raspberry Pi 4, includes a U.FL connector for an external antenna. The "DFRobot IoT Carrier Board Mini" expansion board supplied power and a gigabit Ethernet connection for communication with a host computer. Potential RF leakage from the U.FL connector and adapter cable was identified as a concern. To mitigate this, the units were mounted in shielded enclosures. Raspberry Pi OS Lite version 10 (32-bit, Linux kernel version 5.10.103) was installed on the onboard storage.

The host access point daemon (Hostapd) software was employed on one Raspberry Pi to transmit a service set identifier (SSID), which the second Raspberry Pi used to join the network. The Hostapd (version 2.9) source code was modified to enable 40 MHz bandwidths in the 2.4 GHz band, regardless of any surrounding interference from overlapping stations (technically violating IEEE 802.11-2012, 10.14.3.2). The desired wireless channel was specified, and the HT20 and HT40 capabilities were activated in the Hostapd configuration file. The data rate was measured using the "Iperf3" tool in User Datagram Protocol (UDP) mode, averaging multiple measurements taken over a 60-second duration (block size 1448 bytes).

The radio transmission power and guard interval length were configured in firmware using the "WL" command-line tool from Cypress Semiconductor. We then recorded the auto-negotiated data rate and its corresponding HT MCS setting using Iperf3. Similarly, we recorded the achieved data rate at HT MCS 0-7, with the "WL" tool "forcing" the radio to operate in a specific HT MCS mode. We are currently experimenting with implementing different modulation and synchronization schemes for the transmitting and receiving ends to maximize the throughput and minimize the latency while still ensuring reliable and error-free communication between the two attached boards.

The transceiver implementation will be tested for its performance both when directly connected to a cable and when using the optimized Fat-IBC antennas presented in the previous sections.

5 Experimental setup for Fat-IBC interface testing on Phantoms

Fat-IBC is an innovative approach that enables wireless connections through microwave transmission techniques in and around various human tissues. A primary objective of the B-CRATOS project is to establish a bidirectional wireless communication system linking the brain and a prosthetic arm. The goal is to convey control signals from the motor cortex to the prosthesis and relay sensory data from the arm back to the primary sensory cortex. To achieve this, a two-way communication link with a minimum capacity of 32 Mb/s, ideally 64 Mb/s (brain to prosthesis) and 2 Mb/s (prosthesis to the brain) is required.

Employing Fat-IBC, the only non-proprietary communication technology capable of achieving the necessary speeds for the B-CRATOS project, seems to be wireless LAN (WLAN, based on the IEEE 802.11 group of standards [16]). To attain 64 Mb/s, it is essential to target IEEE 802.11n or higher [19].

This project has received funding from the European Union’s Horizon 2020 research and innovation programme under grant agreement No 965044

The modulation coding scheme (MCS) systems within IEEE 802.11 protocols determine various parameter combinations that result in diverse data rates. The IEEE 802.11n standard outlines eight MCS indices for "high throughput" (HT) data rates with 20 MHz (HT20) and 40 MHz (HT40) channel bandwidths in the 2.45 GHz band. Table I presents the HT data rates (for a single spatial stream with the default 800 ns guard interval). To achieve 64 Mb/s with HT20, the highest modulation rate (64 QAM) and coding are required to surpass 64 Mb/s. Utilizing a 40 MHz bandwidth (HT40) allows reaching such speeds with 16-QAM.

While Fat-IBC's potential for intrabody communication has been demonstrated through small-signal characterization and low-speed data packet transmission, high-speed digital data communication via this link remains unexplored. This paper aims to investigate Fat-IBC as a communication link with both in-body (implanted) and on-body (on the skin) antennas in the 2.4 GHz band within the body, striving to achieve 64 Mb/s end-to-end data communication.

This demonstration uses phantoms with three layers, simulating skin, fat, and muscle, respectively. The phantoms are designed for the frequency range of 500 MHz to 20 GHz and are constructed from semi-solid, low-water content structures intended to mimic the properties of actual human tissues. The muscle and skin layers of the phantoms were produced in a controlled environment. The materials employed included DI water, n-propanol, canola oil, kerosene, gelatin, TX-151, surfactant, glycerine, dextrin, corn starch, salt, and sodium benzoate. Varying material compositions of the layers resulted in diverse dielectric properties, which were assessed using a Keysight 85070E slim probe. The measurements closely aligned with the reference data from the Istituto di Fisica Applicata "Nello Carrara" (IFAC) database for the 2.45 GHz frequency, offering a standard for dielectric properties of biological tissues.

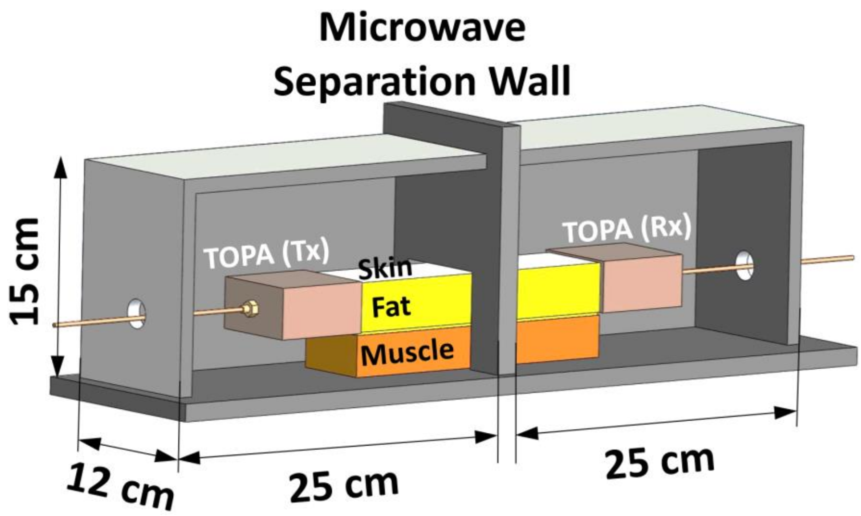

Figure 14. **A conceptual model of the shielded chamber, with two TOPAs and a phantom.**

Due to the low water content of the tissues, the phantoms can be stored for extended periods without drying. For the fat layer, vulcanized rubber with dielectric properties similar to human fat tissue was used, exhibiting a relative permittivity of 5.28 and conductivity of 0.1 S/m.

This project has received funding from the European Union's Horizon 2020 research and innovation programme under grant agreement No 965044

Three-layer phantoms of 10, 20, and 30 cm lengths were created. All phantoms had widths of 58 mm, fat and muscle layer heights of 30 mm each, and an approximate skin layer thickness of 2 mm. These dimensions are comparable to our previous work, with the exception that earlier studies only used phantoms up to 10 cm in length.

5.1 Design of a shielded chamber for phantom measurements

We employed a shielded chamber to minimize external interference, as illustrated in Fig. 14. The chamber features a wall designed to suppress surface waves, primarily at the air-skin interface. Interference from surface waves, which act as secondary (undesired) propagation paths, is anticipated to be more significant for Case 2 and Case 3 due to the on-body antennas. The separation wall effectively reduces such surface waves for all cases.

The chamber comprises two rectangular cuboid-like 3D-printed plastic structures divided by the removable separation wall. All internal surfaces of the cuboids and lateral surfaces of the separation wall are lined with high-loss 15-mm thick foam microwave absorbers (EA-LF500-24). The separation wall has overall dimensions of 18 x 15 x 2.5 cm and extends slightly from the cuboids. A section at the bottom part of the separation wall is tailored to accommodate the three-layer phantom. The chamber's external surfaces are covered with a 30-µm thick aluminum foil to improve shielding efficiency.

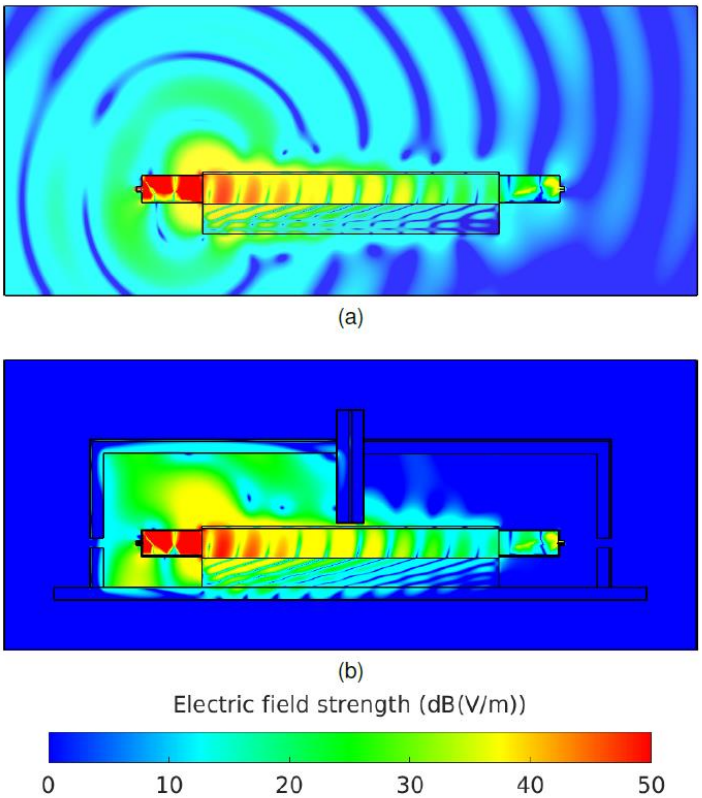

Figure 15. **Longitudinal-cut plane view of the simulated 3D electric field distribution at 2.45 GHz for Case 1 with a 30 cm phantom: (a) without the shielded chamber and wall and (b) with the shielded chamber and wall. The scale is clamped at 0 dB(V/m) and 50 dB(V/m).**

This project has received funding from the European Union's Horizon 2020 research and innovation programme under grant agreement No 965044

To showcase the shielding capability of the chamber, we utilized CST Microwave Studio 2021 to simulate the 3D electric field distribution for two instances of Case 1: one with the shielded chamber and wall and the other without them. The simulations included the TOPAs and a 30-cm phantom and were conducted with an "open" boundary. The phantoms were modeled based on dispersion data from the IFAC database.

Fig. 15 clearly demonstrates the suppression ability of the wall, showcasing the suppression of a space wave and reduction of a surface wave when comparing the shielded and unshielded cases.

5.2 Radio equipment and parameter settings

Using a shielded chamber, different phantoms, and antenna combinations, we evaluated the signal connection from the antennas to the fat channel and the signal losses in the channel. Also, We evaluate scattering parameters (S-Parameters) between 2 and 3 GHz with a Keysight N9918A Fieldfox microwave analyzer.

To evaluate the performance of antennas and fat channels with modulated signals, we employed a Rohde & Schwarz (R&S) SMCV100B vector signal generator (VSG) and an FSVA3000 vector signal and spectrum analyzer (VSA). Measurements of bit error rate (BER) versus normalized SNR (Eb/N0) were utilized to compare the performance of various digital modulation schemes.

A 1 MSamples/s PRBS 9-encoded data stream with an RRC filter setting of 0.22 was applied to all digital modulation formats (BPSK to 512-QAM, with IEEE 802.11n using up to 64-QAM). The output power of the VSG was set to 10 dBm at the 2.45 GHz target frequency. The Eb/N0, using added additive white Gaussian noise (AWGN), was swept, and the BER down to 10^−6 was recorded for the different modulations.

5.2.1 IEEE 802.11n link

For the 802.11n connection, we employed two Raspberry Pi Compute Module 4 units (CM4102008). This specific Raspberry Pi model comes with a wireless module based on the Cypress Semiconductor CYW43455, which, in contrast to the wireless module on the standard Raspberry Pi 4, features a U.FL connector for an external antenna. A "DFRobot IoT Carrier Board Mini" expansion board supplied power and a gigabit Ethernet connection for communication with a host computer.

RF leakage from the U.FL connector and adapter cable was identified as a potential issue. To tackle this, the units were mounted in 3D-printed enclosures wrapped in a 30-μm thick aluminum sheet. Each enclosure was placed on an absorber sheet, with another absorber sheet on top. The U.FL-to-SMA connections were also covered with the aluminum sheet.

Raspberry Pi OS Lite version 10 (32-bit, Linux kernel version 5.10.103) was installed on the onboard storage. The host access point daemon (Hostapd) software was employed on one Raspberry Pi to broadcast a service set identifier (SSID), which the second Raspberry Pi used to join the network. The Hostapd (version 2.9) source code was modified to permit 40 MHz bandwidths in the 2.4 GHz band, irrespective of any surrounding interference from

This project has received funding from the European Union’s Horizon 2020 research and innovation programme under grant agreement No 965044

overlapping stations (technically violating IEEE 802.11-2012, 10.14.3.2). We specified the desired wireless channel and enabled the HT20 and HT40 capabilities in the Hostapd configuration file. The data rate was measured using the "Iperf3" tool in User Datagram Protocol (UDP) mode as an average of multiple measurements conducted over a duration of 60 seconds (block size 1448 bytes).

The radio transmission power and guard interval length were set in firmware using the "WL" command-line tool from Cypress Semiconductor. Afterward, we documented the auto-negotiated data rate and its related HT MCS setting with Iperf3. Similarly, the achieved data rate at HT MCS 0-7 was recorded using the "WL" tool to "force" the radio to operate in a specific HT MCS mode.

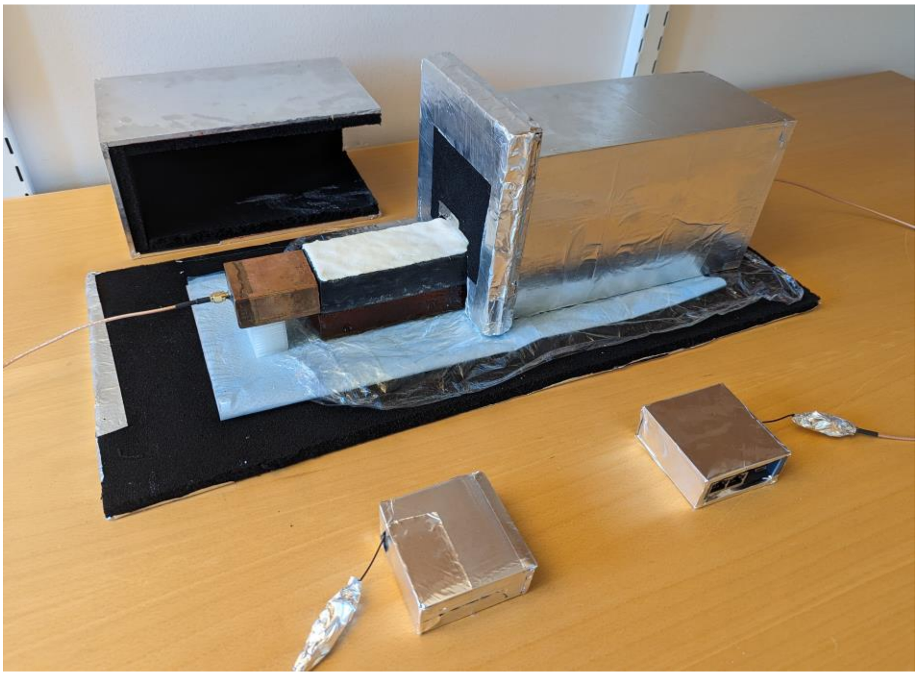

Figure 16. **The shielded chamber with one chamber segment at the side, exposing the three-layer phantom and one of the TOPAs inside. In front are the two Raspberry Pis inside aluminum-clad cases.**

The efficacy of the Fat-IBC link for high-speed data transmission is assessed using various antenna configurations. This is done by conducting s-parameter measurements, modulating high-speed data tests, and establishing a WLAN link through the Fat-IBC material utilizing two Raspberry Pis connected to the in-body and on-body antennas. All radio experiments employ the same equipment setup, which includes phantoms and a shielded chamber, differing only in the length of the phantoms (10, 20, 30 cm) and the antenna combinations (in-body and on-body). Fig.18 illustrates the actual measurement configuration, showcasing the shielded chamber (opened for inspection purposes), a phantom, and a TOPA.

This project has received funding from the European Union's Horizon 2020 research and innovation programme under grant agreement No 965044

5.2.2 Inbody-to-inbody antennas

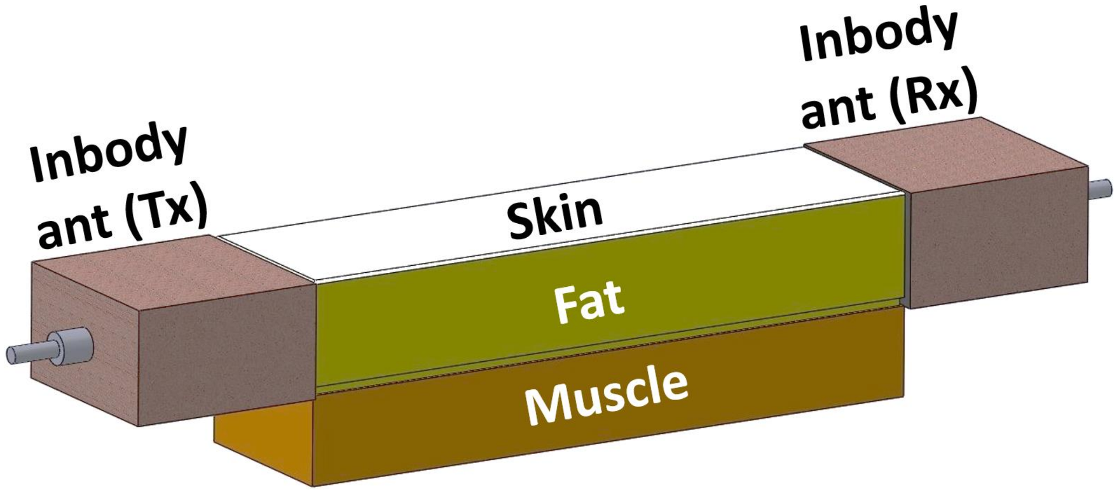

Figure 17. **Inbody-to Inbody antennas**

Fig. 18, parts (a) and (b), exhibit the measured input (S_{11}) and output (S_{22}) reflection coefficients for the implant-to-implant antenna configuration. The values below -25 dB signify an exceptional coupling of the signal into the fat layer for the 10 cm and 20 cm phantoms. For the 30 cm phantom, the S_{11} and S_{22} values are slightly higher but remain below -15 dB. Given that the phantoms do not have a 50 Ω impedance, this could imply a marginally greater mismatch compared to the shorter phantoms.

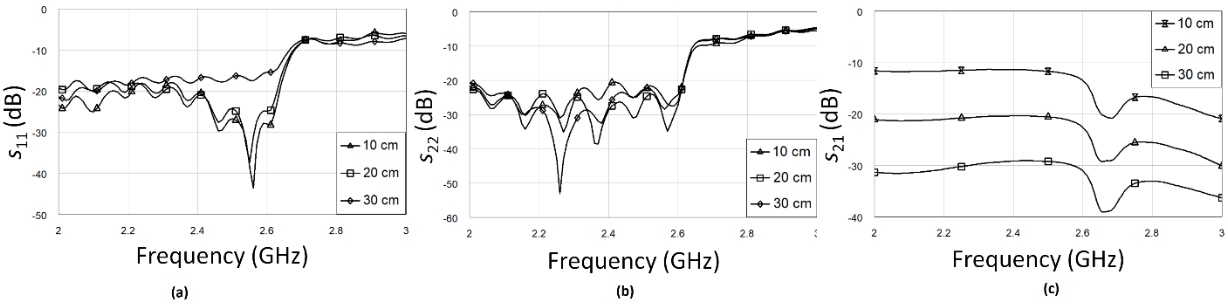

Figure 18. **(a) input reflection coefficient (S_{11}), (b) output reflection coefficient (S_{22}), (c) transmission coefficient (S_{21}) for the three different phantom lengths.**

Fig. 18 (c) displays the transmission coefficient (S_{21}), which scales almost linearly (in dB) as 1 dB/cm loss at the target frequency of 2.45 GHz, in line with our earlier observations.

The radio link performance, assessed as outlined in Section II-D, for various modulation schemes, is shown in Fig.6 for the 30 cm phantom (the shorter phantoms exhibited nearly identical performance). We achieved a BER < 10^{-6} for all tested modulations.

This project has received funding from the European Union's Horizon 2020 research and innovation programme under grant agreement No 965044

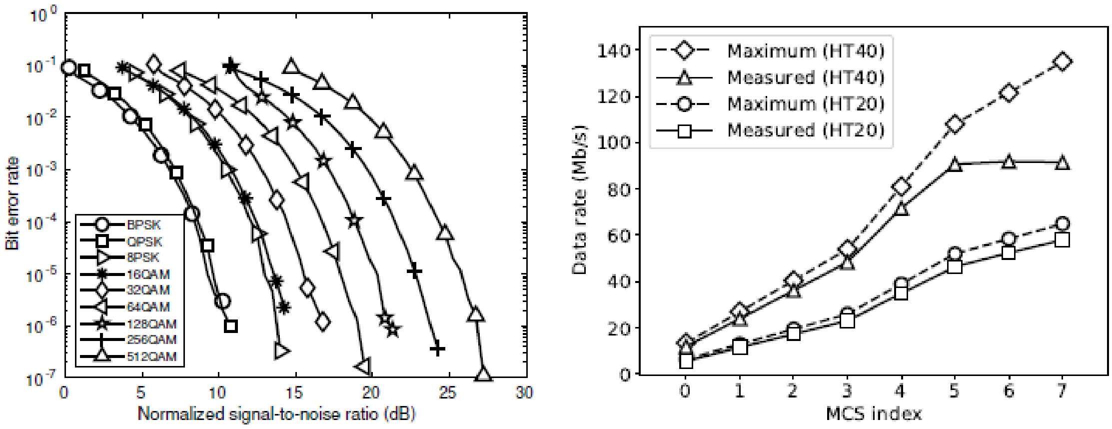

(a) (b)

Figure 19. **(a)BER vs. Eb/N0 for different modulations schemes (b) Date rate vs. MCS index for bandwidths of 20 MHz and 40 MHz, 30 cm phantom length**

To evaluate the performance using a recognized wireless communication standard and tools, we measured the fat-channel link performance with an IEEE 802.11n network as detailed in Section II-E. By connecting the two Raspberry Pis to different antenna combinations, a local auto-negotiating peer-to-peer network was established. For the 30 cm phantom with the implanted antennas inside the shielded chamber, we achieved a 91.6 Mb/s link (MCS 7, HT40).

We also conducted an MCS sweep, enforcing the modulation settings for 20 and 40 MHz bandwidths. The resulting data rates are presented in Fig. 7. For a 20 MHz bandwidth, we achieved up to 58.0 Mb/s, while increasing the bandwidth to 40 MHz led to a data rate saturation at 92 Mb/s for MCS 5–7 (64-QAM).

5.2.3 Inbody-to-on-body antennas:

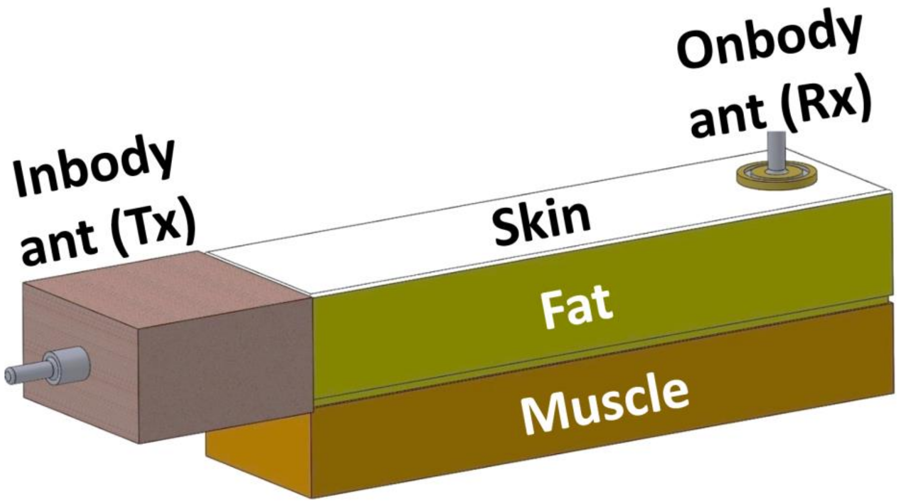

Figure 20. **Inbody-to-Onbody antennas**

Fig. 21 presents the measured S_{11} and S_{22} parameters for the in-body-to-on-body antenna configuration. The input (S_{11}) and output (S_{22}) reflection coefficients are now asymmetrical, exhibiting high reflection coefficients for port 2, which is the on-body antenna. The S_{11}

This project has received funding from the European Union's Horizon 2020 research and innovation programme under grant agreement No 965044

indicates a favorable coupling using the implanted antenna (less than -15 dB), while the S_{22}, the on-body antenna, demonstrates reduced coupling (-4 dB) to the fat layer. The S_{21}, shown in Fig. 21(c), displays losses at 2.45 GHz corresponding to the phantom lengths, similar to the in-body-to-in-body antennas, but with higher fixed losses due to the less optimal coupling (S_{22}) from the on-body antenna to the phantom.

The radio link performance, depicted in Fig. 22, is nearly identical to the implant-to-implant case, although at 512-QAM, the performance declines at low BER levels.

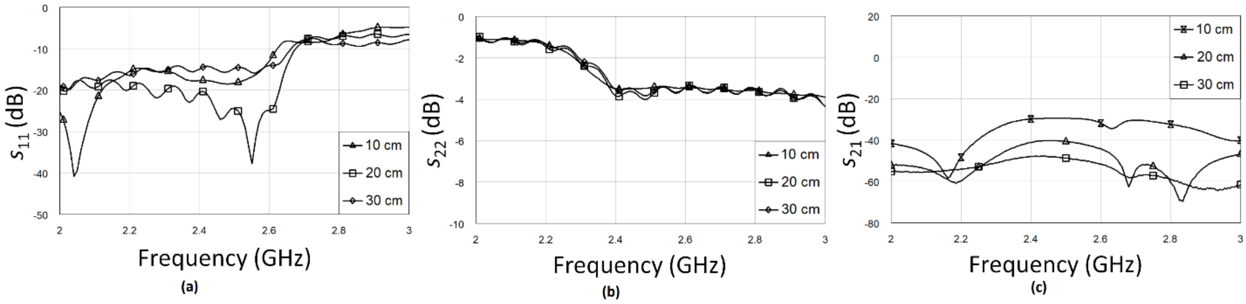

Figure 21. **inbody-to-onbody antennas: (a) input reflection coefficient(S_{11}), (b) output reflection coefficient (S_{22}), (c) transmission coefficient (S_{21}) for the three different phantom lengths.**

The radio link performance, as shown in Fig.22, is nearly indistinguishable from the implant-to-implant scenario, although at 512-QAM, the performance declines at low BER levels. When connecting the two Raspberry Pis to the in-body/on-body antennas, a nearly identical link speed of 91.8 Mb/s (MCS 7, HT40) to the in-body-to-in-body case (91.6 Mb/s) was achieved.

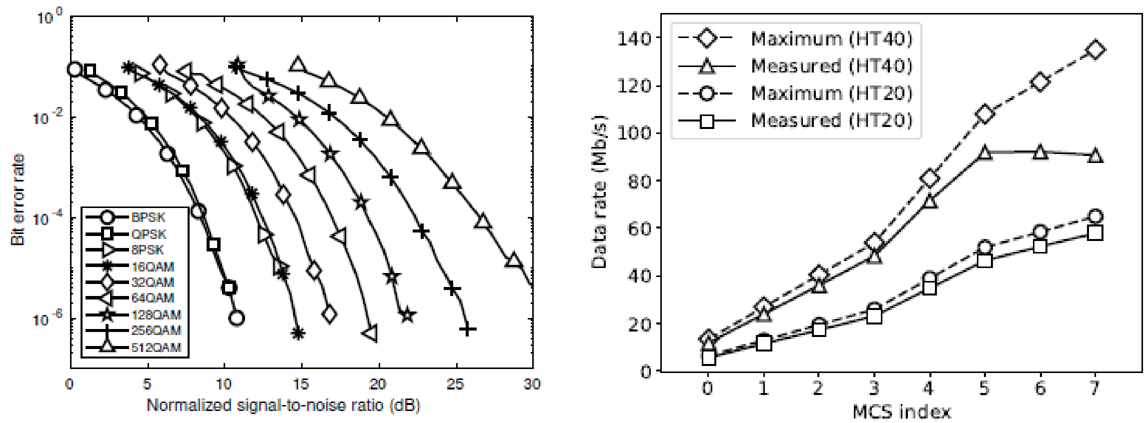

Figure 22. **(a)BER vs. Eb/N0 for different modulations schemes (b) Date rate vs. MCS index for bandwidths of 20 MHz and 40 MHz, 30 cm phantom length**

Examining the MCS for 20 and 40 MHz bandwidth, as illustrated in Fig.22, reveals a performance comparable to the prior case, with nearly 60 Mb/s performance for 20 MHz bandwidth and approximately 92 Mb/s using MCS 5–7 (64-QAM) at 40 MHz bandwidth.

This project has received funding from the European Union's Horizon 2020 research and innovation programme under grant agreement No 965044

5.2.4 Onbody-to-onbody antennas

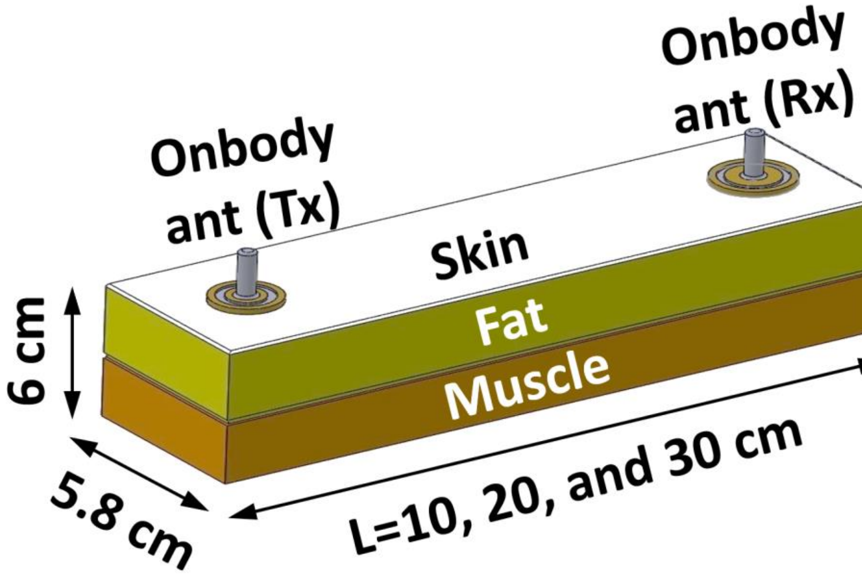

Figure 23. **onbody-to-onbody antennas**

The s-parameters for the scenario with dual on-body antennas demonstrate suboptimal coupling to the skin/fat/muscle phantom, as evidenced in Fig. 23. This also eliminates potential variations in matching to different phantoms with varying lengths. The S_{21}, shown in Fig. 23(b), exhibits a reasonable correlation with the phantom length.

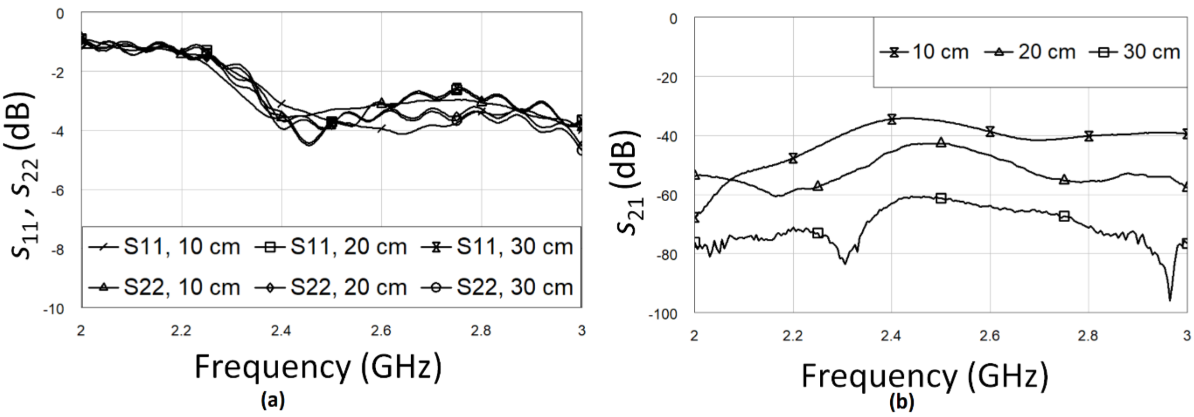

Figure 24. **onbody-to-onbody antennas: (a) input reflection coefficient (s11) and output reflection coefficient (S_{22}), (b) transmission coefficient (S_{21}) for the three different phantom lengths.**

The radio link performance depicted in Fig. 25(c) displays a noticeable degradation of BER with the 30 cm phantom for 32-QAM and higher-order modulations. In contrast, the 20 cm phantom, illustrated in Fig. 25(b), reveals some decline for 128-QAM and higher modulations, while the 10 cm phantom, demonstrated in Fig. 25(a), presents satisfactory performance for all modulations. Considering the losses in the link through various phantoms and the settings of the signal analyzer during measurements, this degradation is likely attributed to an insufficient input signal for the analyzer to demodulate the received signals accurately.

This project has received funding from the European Union’s Horizon 2020 research and innovation programme under grant agreement No 965044

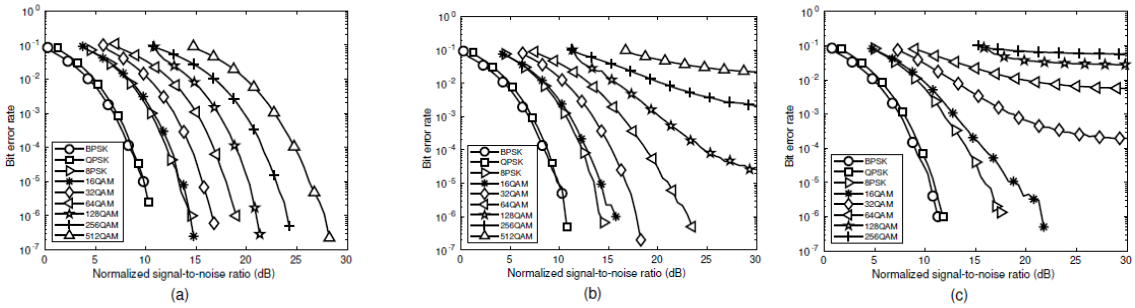

Figure 25. **BER vs. Eb/N0 for different modulation schemes:(a) 10 cm phantom length, (b) 20 cm phantom length, (c) 30 cm phantom length.**

Concerning the Raspberry Pi link speed, in this case, it was also feasible to achieve a link speed of 91.6 Mb/s (MCS 7, HT40). Examining the MCS for 20 and 40 MHz bandwidth, as portrayed in Fig. 23, reveals performance similar to the previous instances, with 58 Mb/s performance for 20 MHz bandwidth and 92 Mb/s employing MCS 5–7 (64-QAM) at 40 MHz bandwidth.

5.3 Achievement from Experiment

The small-signal analysis of the phantoms with various antenna combinations indicates a loss for microwave signals of approximately 1 dB/cm in the fat channel. The in-body antennas provide exceptional coupling to the fat channel, while the on-body (on the skin) antennas necessitate improvements to better couple the signal to/from the fat channel without significant insertion losses.

The BER measurements illustrate that, excluding the use of dual on-body antennas with longer phantoms, the Fat-IBC link is highly linear and capable of handling modulations as intricate as 512-QAM without any degradation of the BER. Concerning high-speed data communication, the throughput plateaus at 92 Mb/s for all distinct phantoms and antenna combinations. This is not the upper limit according to the IEEE 802.11n standard (see Table I), but the throughput is likely restricted by the SDIO interface on the CYW43455 wireless module. The findings demonstrate that a Fat-IBC link, utilizing low-cost, off-the-shelf hardware and established IEEE 802.11 wireless communication, can attain high-speed data communication within the body. The data rate is among the fastest measured with intra-body communication, as shown in Table II, which compares other similar in-body communication methods.

In the case of on-body antennas using the longest 30 cm phantom, the WLAN link speed of 92 Mb/s data with 64-QAM modulation at 40 MHz bandwidth was still achieved, despite the anticipated degradation in the full link speed based on the BER measurements plot (Fig. 25(a)). The BER measurements (refer to Section II-D) were conducted using a generic 1 MS/s data stream without any sophisticated coding or error correction typically present in an actual IEEE 802.11n system. Consequently, the BER results might not provide a clear indication of the achievable data rate when used with a comprehensive IEEE 802.11n system.

For the utilized phantoms and antennas, no limitations in the obtained link speed for IEEE 802.11n correlated to the antennas or the length of the phantoms were observed. By using only in-body antennas, 30 dB is gained in the link budget compared to on-body antennas,

This project has received funding from the European Union's Horizon 2020 research and innovation programme under grant agreement No 965044

extending the possible link distance by 30 cm. Since the losses are proportional to the phantom length, increasing the transmitted power may proportionally extend the fat channel length without degrading the throughput while considering applicable specific absorption rate (SAR) limitations.

6 Conclusion

In this report, we have discussed the transceiver module and front end dedicated to the B-CRATOS project. Additionally, experiments were carried out using different combinations to explore the potential of Fat Intra-Body Communication (Fat IBC) systems for high-speed data transmission within the human body, making it a promising solution for intrabody communication applications. We successfully evaluated the signal coupling and losses through the fat channel by utilizing various antenna combinations, including in-body (implanted) and on-body (on the skin) antennas, phantoms, and a shielded chamber.

The Fat IBC system was characterized using S-parameter measurements, and Bit Error Rate (BER) measurements were employed to compare the performance of different digital modulation schemes. To achieve a target data rate of 64 Mb/s, we implemented IEEE 802.11n wireless communication in the 2.4 GHz band to establish a link inside the body, which was emulated by phantoms of varying lengths.

For all antenna combinations and phantom lengths, link speeds of 92 Mb/s were achieved using the 40 MHz bandwidth provided by the IEEE 802.11n standard. This speed is most likely limited by the radio circuits used rather than the Fat IBC link itself. The use of 3D-printed housing with absorbers further contributed to reducing back radiation and ensuring efficient data transfer through the fat channel.

This project has received funding from the European Union's Horizon 2020 research and innovation programme under grant agreement No 965044

7 Revision history

REVISIONS			
Version #	**Date**	**Type of Change**	**Lead Author**
1.1	01-04-2023	First draft Started	Bappaditya Mandal
1.2	15-04-2023	Added Transceiver part in the draft	Bappaditya Mandal
1.3	28-04-2023	Contributions from Fondazione LINKS	Rossella Gaffoglio
1.4	29-04-2023	Final draft and sent to Group leader for comments	Bappaditya Mandal
1.5	29-04-2023	Review by WPL	Robin Augustine

This project has received funding from the European Union's Horizon 2020 research and innovation programme under grant agreement No 965044